Available online at www.sciencedirect.com

ScienceDirect

IFAC Papers Online CONFERENCE PAPER ARCHIVE

IFAC PapersOnLine 50-1 (2017) 4660–4665

Robust Multi-Parametric Control of Continuous-Time Linear Dynamic Systems

Muxin Sun [*,**] **Mario E. Villanueva** [**]
Efstratios N. Pistikopoulos [**] **Benoît Chachuat** [*]

[*] *Centre for Process Systems Engineering, Department of Chemical Engineering, Imperial College London, London, SW7 2AZ, UK.*
[**] *Artie McFerrin Department of Chemical Engineering, Texas A&M University, College Station, TX 77843, USA.*

Abstract: We extend a recent methodology called multi-parametric NCO-tracking for the design of parametric controllers for continuous-time linear dynamic systems in the presence of uncertainty. The approach involves backing-off the path and terminal state constraints based on a worst-case uncertainty propagation determined using either interval analysis or ellipsoidal calculus. We address the case of additive uncertainty, and we discuss approaches to handling multiplicative uncertainty that retain tractability of the mp-NCO-tracking design problem, subject to extra conservatism. These developments are illustrated with the case study of a fluidized catalytic cracking (FCC) unit operated in partial combustion mode.

Keywords: Robust model predictive control; Constrained linear-quadratic regulation; Multi-parametric programming; Multi-parametric NCO-tracking.

1. INTRODUCTION

On-line optimization and real-time control have received much attention over the past few decades, driven by the need to improve performance and reduce economic costs in industrial processes. The strategy employed in classical model predictive control (MPC) entails the repeated solution of an optimal control problem that predicts the system's future behavior over a finite, receding time-horizon, using the current state measurements or estimates as initial conditions (Rawlings and Mayne, 2009). The optimized control strategy is implemented until the next measurements become available, and it is the repetition of this process that creates a feedback control.

Several approaches have been proposed in the literature to mitigate the computational burden associated to the online solution of optimization problems in MPC. In the multi-parametric programming paradigm (Pistikopoulos, 2012), the optimization is performed off-line, resulting in an explicit mapping of the control strategies as a function of the initial state. For continuous-time systems, this approach gives rise to multi-parametric dynamic optimization (mp-DO) problems, which may either be transformed into finite-dimensional multi-parametric programs via full discretization (direct approach), or handled directly using optimal control theory (indirect approach).

Another approach to reducing the computational burden in MPC, involves tracking the necessary conditions for optimality (NCO), namely *NCO-tracking* (Kadam et al., 2007; Bonvin and Srinivasan, 2013). In continuous time, NCO-tracking starts by characterizing the optimal switching structure of the control trajectories. Under the assumption that this switching structure remains unchanged in the presence of uncertainty, feedback laws are then constructed for tracking the active constraints and zero gradient conditions along each arc.

The so-called multi-parametric (mp-)NCO-tracking approach was introduced by Sun et al. (2016). It combines mp-DO and NCO-tracking into a unified framework for multi-parametric MPC via the indirect approach. An algorithm for characterizing the corresponding multi-parametric solution structure in terms of the exact critical regions and nonlinear feedback control laws was proposed for linear-quadratic optimal control problems. In essence, mp-NCO-tracking provides a means of relaxing the invariant switching-structure and active-set assumptions in NCO-tracking by constructing critical regions for each switching structure, while enabling a reduction in the number of critical regions compared to direct mp-MPC approaches.

The implementation of MPC controllers, both classical and multi-parametric, is based on a certainty-equivalence principle, whereby the future of the system is optimized as if neither external disturbances nor model mismatch were present, despite the fact that such disturbances and mismatch are the reason why feedback is needed in the first place. This approach works well in many practical applications, and it often exhibits a certain robustness due to its inherent ability to reject disturbances. When large disturbances occur, the constraints can nonetheless become violated, thereby calling for the development of robust MPC schemes (Bemporad and Morari, 1999; Sakizlis et al., 2004; Kouramas et al., 2013).

This paper extends the mp-NCO-tracking approach in order to enable robust multi-parametric controllers for continuous-time linear dynamic systems. This approach is inspired by tube-based MPC, and in particular the so-called rigid tube MPC approach (Mayne, Seron and

2405-8963
10.1016/j.ifacol.2017.08.690

Raković, 2005). It involves backing-off the path and terminal state constraints based on a worst-case uncertainty propagation determined using either interval analysis or ellipsoidal calculus. In particular, special attention is paid to retaining the tractability of the mp-NCO-tracking design problem. The rest of the paper is organized as follows: Sect. 2 formulates the optimal control problem of interest; Sect. 3 provides some background on mp-NCO-tracking controllers; Sect. 4 develops robust mp-NCO-tracking controllers based on a robust-counterpart formulation of the mp-DO problem and considers both additive and multiplicative time-varying uncertainty; results for the numerical case study of a fluidized catalytic cracking (FCC) unit are presented in Sect. 5; finally, Sect. 6 concludes the paper.

2. PROBLEM FORMULATION

We consider constrained linear-quadratic optimal control problems under uncertainty, in the form:

$$\begin{aligned} \inf_{x,u} \;& \frac{1}{2}\int_0^T x(t)^\mathsf{T} Q x(t) + u(t)^\mathsf{T} R u(t)\;\mathrm{d}t + \frac{1}{2}x(T)^\mathsf{T} Q_\mathrm{f} x(T) \\ \text{s.t.}\;& \dot{x}(t) = F_x x(t) + F_u u(t) + F_\theta \theta + F_w w(t) + f_0 \\ & x(0) = B_0\theta + b_0 \\ & G_x x(t) + G_u u(t) + G_\theta \theta + g_0 \le 0 \\ & H_x x(T) + H_\theta \theta + h_0 \le 0\,. \end{aligned} \tag{1}$$

Besides standard notation in Appendix A, $x \in \mathbb{W}^{n_x}_{1,2}$ denote the state response; $u \in \mathcal{U} := \{u \in \mathbb{L}^{n_u}_2 \,|\, \forall t \in [0,T], u(t) \in U\}$ with $U \in \mathbb{K}^{n_u}_\mathrm{C}$, the control input; $\theta \in \mathbb{K}^{n_\theta}_\mathrm{C}$, the problem parameters; $w \in \mathcal{W} := \{w \in \mathbb{L}^{n_w}_2 \,|\, \forall t \in [0,T], w(t) \in W\}$ with $W \in \mathbb{K}^{n_w}_\mathrm{C}$, the time-varying uncertainty; and $Q_\mathrm{f} \succeq 0$, $Q \succeq 0$, and $R \succ 0$ are given weighting matrices.

The focus of the paper is on constructing robust mp-NCO-tracking controllers, which can guarantee feasibility in the worst-case scenario for the time-varying uncertainty $w(t)$. The objective is to develop robust formulations that are amenable to numerical solution with the same computational effort as the nominal mp-NCO-tracking controllers in Sun et al. (2016), i.e. with $F_w = 0$.

3. mp-NCO-TRACKING METHODOLOGY

For a given parameter value θ and in the absence of uncertainty, the optimal feedback control trajectory $u(t)$ for problem (1) consists of a finite sequence of $N_t(\theta)$ arcs, which define the so-called optimal switching structure denoted by $\mathcal{S}(\theta)$. The switching times $t_k(\theta)$, $k = 1 \dots N_t(\theta)-1$, between adjacent arcs either correspond to the activation or deactivation time for a given path constraint, or touch-and-go points in the case of higher-order state constraints. Besides their switching structure, characterizing an optimal solution involves determining the 6-tuple $(u(t), x(t), \lambda(t), \mu(t), \nu, \pi)$, where $\lambda(t) \in \mathbb{R}^{n_x}$ are the costate (adjoint) variables; $\mu(t) \in \mathbb{R}^{n_g}$, the multipliers for the path constraints; $\nu \in \mathbb{R}^{n_h}$, the multipliers for the terminal constraints; and π are extra multipliers for certain interior-point constraints in the presence of high-order state constraints.

The mp-NCO-tracking methodology by Sun et al. (2016) proceeds in two steps, as illustrated in Fig. 1:

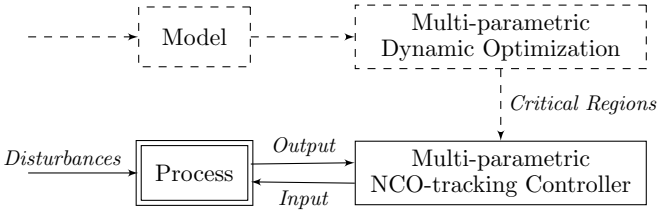

Fig. 1. Principle of multi-parametric NCO tracking.

- The first (off-line) step defines the multi-parametric control structure, which entails a partitioning of the uncertain parameter domain into NC critical regions, $\Theta^1 \cup \dots \cup \Theta^{NC} \subseteq \Theta$, each corresponding to a unique switching structure $\mathcal{S}^1, \dots, \mathcal{S}^{NC}$. Moreover, mp-DO determines parametric optimal solution in the form:
$$\forall \theta \in \Theta^i, \quad (u(t), x(t), \lambda(t), \mu(t), \nu, \pi) = \mathcal{K}^i\left(t, \theta, t^i_1(\theta), \dots, t^i_{N^i_t-1}(\theta)\right),$$
for each $i = 1 \dots NC$, where the junction times $t^{(i)}_k$ themselves are dependent on θ.
- The subsequent (on-line) step applies the multi-parametric NCO-tracking controller in a receding horizon manner. This step involves determining the critical region Θ^i containing the current parameter values θ, by testing primal and dual feasibility under the corresponding feedback laws $\mathcal{K}^i$. It also involves computing the current junction times $t^{(i)}_k$, for instance by using a Newton iteration. Then, the selected feedback laws are implemented until new measurements become available at the next sampling time.

4. ROBUST mp-NCO-TRACKING CONTROLLERS

This section develops a robustification of the mp-NCO-tracking methodology by Sun et al. (2016), whereby worst-case uncertainty propagation (Chachuat et al., 2015) is applied to back-off the terminal and path constrained in order for the feedback controller to guarantee feasibility under all possible uncertainty scenarios.

We proceed by splitting the state and the disturbance into nominal and perturbed components as

$$x(t) = \hat{x}(t) + d_x(t)\,, \qquad w(t) = \hat{w} + d_w(t)\,, \tag{2}$$

for a given $\hat{w} \in W$ and $\hat{x}$ such that

$$\begin{aligned} & \dot{\hat{x}}(t) = F_x \hat{x}(t) + F_u u(t) + F_\theta \theta + F_w \hat{w} + f_0 \\ & \text{with} \quad \hat{x}(0) = B_0\theta + b_0\,. \end{aligned}$$

It follows that the dynamics of the state perturbation d_x, given by

$$\begin{aligned} & \dot{d}_x(t) = F_x d_x(t) + F_w d_w(t) \\ & \text{with} \quad d_x(0) = 0\,, \end{aligned} \tag{3}$$

is independent of both the control u and the parameter θ. A unique solution to the initial value problem (3) exists for all $w \in \mathcal{W}$, denoted by $\delta(\cdot, w)$ subsequently, and the reachability tube $\Delta : [0,T] \to \mathbb{K}^{n_x}$ describing the solution set of (3) for all possible realizations of the time-varying uncertainty w is given by

$$\Delta(t) := \{d \in \mathbb{R}^{n_x} \,|\, \exists w \in \mathcal{W} :\; d = \delta(t,w)\}\,. \tag{4}$$

Then, following Houska et al. (2012), a conservative robust counterpart to the problem (1) that minimizes the nominal cost can be stated as

$$\begin{aligned}\inf_{\hat{x},u}\ & \frac{1}{2}\int_0^T \hat{x}(t)^\mathsf{T} Q \hat{x}(t) + u(t)^\mathsf{T} R u(t)\ \mathrm{d}t + \frac{1}{2}\hat{x}(T)^\mathsf{T} Q_\mathrm{f} \hat{x}(T)\\ \text{s.t.}\ & \dot{\hat{x}}(t) = F_x \hat{x}(t) + F_u u(t) + F_\theta \theta + F_w \hat{w} + f_0\\ & \hat{x}(0) = B_0\theta + b_0\\ & \max_{\delta\in\overline{\Delta}(t)} G_x[\hat{x}(t)+\delta] + G_u u(t) + G_\theta\theta + g_0 \le 0\\ & \max_{\delta\in\overline{\Delta}(T)} H_x[\hat{x}(T)+\delta] + H_\theta\theta + h_0 \le 0\,,\end{aligned} \tag{5}$$

where $\overline{\Delta}(t) \supseteq \Delta(t)$ stands for any compact enclosure of the reachable set on $[0,T]$. An inherent advantage of this formulation is that the developments in Sun et al. (2016) apply readily to the problem (5) in order to devise a robust mp-NCO-tracking controller.

Generally, any convex set-valued function $\overline{\Delta} : [0,T] \to \mathbb{K}_\mathrm{C}^{n_x}$ satisfying the generalized differential inequality

$$\begin{aligned}&\text{a.e. } t\in[0,T],\quad \forall c\in\mathbb{R}^{n_x},\\ &\dot{V}[\overline{\Delta}(t)](c) \ge \max_{d,w}\left\{ c^\mathsf{T}(F_x d + F_w w) \,\middle|\, \begin{array}{l} c^\mathsf{T} d = V[\overline{\Delta}(t)](c)\\ d\in\overline{\Delta}(t)\\ w\in W\end{array}\right\}\\ &\text{with}\quad V[\overline{\Delta}(0)](c)\ge 0\,,\end{aligned}$$

may provide the required enclosures of the reachable tube (4) (Villanueva et al., 2015a). The following two subsections specialize these enclosures to tractable interval and ellipsoidal reachability tubes. We also discuss an extension of the approach to handle multiplicative uncertainty in the dynamic system.

4.1 Case of Interval Reachability Tubes

An interval enclosure $\overline{\Delta}(t) := \left[\delta_x^\mathrm{L}(t), \delta_x^\mathrm{U}(t)\right] \supseteq \Delta(t)$ can be precomputed via the following system of auxiliary ODEs:

$$\begin{aligned}&\text{a.e. } t\in[0,T],\quad \forall i\in 1,\dots,n_x,\\ &\dot{\delta}_{x_i}^\mathrm{L}(t) = \min_{d_x}\left\{ F_{x(i,\cdot)} d_x \,\middle|\, \begin{array}{l} d_{x_i} = \delta_{x_i}^\mathrm{L}(t)\\ d_x\in\overline{\Delta}(t)\end{array}\right\}\\ &\qquad\qquad + \min_{d_w}\left\{ F_{w(i,\cdot)} d_w \,\middle|\, d_w\in\Gamma\right\}\\ &\dot{\delta}_{x_i}^\mathrm{U}(t) = \max_{d_x}\left\{ F_{x(i,\cdot)} d \,\middle|\, \begin{array}{l} d_{x_i} = \delta_{x_i}^\mathrm{U}(t)\\ d_x\in\overline{\Delta}(t)\end{array}\right\}\\ &\qquad\qquad + \max_{d_w}\left\{ F_{w(i,\cdot)} d_w \,\middle|\, d_w\in\Gamma\right\}\\ &\text{with}\quad \delta_{x_i}^\mathrm{L}(0) = \delta_{x_i}^\mathrm{U}(0) = 0 \quad\text{and}\quad \Gamma := W\ominus\{\hat{w}\}\,.\end{aligned}$$

It follows that the robust counterpart problem (5) can be rewritten as

$$\begin{aligned}\inf_{\hat{x},u}\ & \frac{1}{2}\int_0^T \hat{x}(t)^\mathsf{T} Q \hat{x}(t) + u(t)^\mathsf{T} R u(t)\ \mathrm{d}t + \frac{1}{2}\hat{x}(T)^\mathsf{T} Q_\mathrm{f} \hat{x}(T)\\ \text{s.t.}\ & \dot{\hat{x}}(t) = F_x \hat{x}(t) + F_u u(t) + F_\theta \theta + F_w \hat{w} + f_0\\ & \hat{x}(0) = B_0\theta + b_0\\ & G_x\hat{x}(t) + G_u u(t) + G_\theta\theta + g_0 \le -\delta_G(t)\\ & H_x[\hat{x}(T)+\delta] + H_\theta\theta + h_0 \le -\delta_H\,,\end{aligned} \tag{6}$$

with the back-offs $\delta_G(t)$, $0\le t\le T$, and δ_H taken as

$$\begin{aligned}\delta_{G_i}(t) &:= \mathrm{abs}\left(G_{x(i,\cdot)}\right)\ \mathrm{rad}\left(\overline{\Delta}(t)\right),\\ \delta_{H_i} &:= \mathrm{abs}\left(H_{x(i,\cdot)}\right)\ \mathrm{rad}\left(\overline{\Delta}(T)\right).\end{aligned}$$

4.2 Case of Ellipsoidal Reachability Tubes

An ellipsoidal tube enclosure $\overline{\Delta}(t) := \mathcal{E}(Q_x(t)) \supseteq \Delta(t)$ parameterized by the matrix-valued function $Q_x : [0,T] \to \mathbb{S}_+^{n_x}$ can be precomputed by solving the auxiliary ODEs:

$$\begin{aligned}&\text{a.e. } t\in[0,T],\\ &\dot{Q}_x(t) = F_x Q_x(t) + Q_x(t) F_x^\mathsf{T} + \kappa(t) Q_x(t)\\ &\qquad + \frac{1}{\kappa(t)} F_w Q_w F_w^\mathsf{T}\\ &\text{with}\quad Q_x(0) = 0\,,\end{aligned}$$

where we have assumed that the time-varying uncertainty $w(t)$ is in the ellipsoid $\mathcal{E}(\hat{w}, Q_w)$ for all t; and for any given function $\kappa : [0,T] \to \mathbb{R}_{++}$, e.g., so chosen as to minimize the trace of $\dot{Q}_x(t)$,

$$\kappa(t) := \sqrt{\frac{\mathrm{Tr}\left(F_w Q_w F_w^\mathsf{T}\right)}{\mathrm{Tr}\left(Q_x(t)\right) + \epsilon}},$$

for some finite tolerance $\epsilon > 0$.

This way, another choice for the back-offs $\delta_G(t)$, $0\le t\le T$, and δ_H in the robust counterpart problem (6) is

$$\begin{aligned}\delta_{G_i}(t) &:= \sqrt{G_{x(i,\cdot)} Q_x(t) G_{x(i,\cdot)}^\mathsf{T}}\,,\\ \delta_{H_i} &:= \sqrt{H_{x(i,\cdot)} Q_x(t) H_{x(i,\cdot)}^\mathsf{T}}\,.\end{aligned}$$

In practice, the choice of ellipsoidal reachable tubes instead of interval tubes may be dictated by the fact that the former are more efficient at mitigating the wrapping effect, thereby reducing the overall conservatism.

4.3 Extension to Multiplicative Uncertainty

Next, we consider the broader class of uncertain dynamic systems in the form

$$\dot{x}(t) = (F_x + \Omega(t))x(t) + F_u u(t) + F_\theta\theta + F_w w(t) + f_0\,,$$

where the matrix $\Omega(t) := \sum_{j=1}^p K^j w_j(t)$ are uncertain, with given scaling matrices $K^1,\dots,K^p$. A further extension to problems where the matrices F_u and F_θ are also affected by uncertainty is possible, for instance by invoking similar arguments as in Smith (2004).

Applying a similar splitting of the state and the disturbance into nominal and perturbed components as in (2) and $\Omega(t) = \hat{\Omega} + d_\Omega(t)$, we can define the state reference as

$$\begin{aligned}&\dot{\hat{x}}(t) = (F_x + \hat{\Omega})\hat{x}(t) + F_u u(t) + F_\theta\theta + F_w\hat{w} + f_0\\ &\text{with}\quad \hat{x}(0) = B_0\theta + b_0\,.\end{aligned}$$

The dynamics of the state perturbation d_x become

$$\begin{aligned}\dot{d}_x(t) &= (F_x + \hat{\Omega})d_x(t) + d_\Omega(t)(\hat{x}(t) + d_x(t))\\ &\quad + F_w d_w(t)\\ &\text{with}\quad d_x(0) = 0\,,\end{aligned} \tag{7}$$

and are now dependent on the control u and the parameter θ via the nominal state trajectory $\hat{x}$. Therefore, a similar strategy as for additive uncertainty, whereby reachability tubes can be precomputed for the state disturbances, will rely on the availability of a conservative enclosure $\hat{X}(t) \in \mathbb{K}^{n_x}$ for the nominal state. For instance, such enclosures can be obtained using state-of-the-art set-valued integrators (Houska et al., 2012; Chachuat et al., 2015).

Here, an interval tube enclosure $\overline{\Delta}(t) := \left[\delta_x^{\mathrm{L}}(t), \delta_x^{\mathrm{U}}(t)\right] \supseteq \Delta(t)$ can be precomputed by solving the auxiliary ODEs:

$$\text{a.e. } t \in [0,T], \quad \forall i \in 1,\dots,n_x,$$

$$\dot{\delta}_{x_i}^{\mathrm{L}}(t) = \min_{\substack{d_x, d_w, \\ \hat{x}}} \left\{ \left(F_{x(i,\cdot)} + \sum_{j=1}^{p} K_{(i,\cdot)}^{j} \hat{w} \right) d_x + \sum_{j=1}^{p} K_{(i,\cdot)}^{j} d_{w_j} (\hat{x} + d_x) + F_{w(i,\cdot)} d_w \;\middle|\; \begin{array}{l} d_{x_i} = \delta_{x_i}^{\mathrm{L}}(t) \\ d_x \in \overline{\Delta}(t) \\ \hat{x} \in \hat{X}(t) \\ d_w \in \Gamma \end{array} \right\}$$

$$\dot{\delta}_{x_i}^{\mathrm{U}}(t) = \max_{\substack{d_x, d_w, \\ \hat{x}}} \left\{ \left(F_{x(i,\cdot)} + \sum_{j=1}^{p} K_{(i,\cdot)}^{j} \hat{w} \right) d_x + \sum_{j=1}^{p} K_{(i,\cdot)}^{j} d_{w_j} (\hat{x} + d_x) + F_{w(i,\cdot)} d_w \;\middle|\; \begin{array}{l} d_{x_i} = \delta_{x_i}^{\mathrm{U}}(t) \\ d_x \in \overline{\Delta}(t) \\ \hat{x} \in \hat{X}(t) \\ d_w \in \Gamma \end{array} \right\}$$

$$\text{with} \quad \delta_{x_i}^{\mathrm{L}}(0) = \delta_{x_i}^{\mathrm{U}}(0) = 0\,.$$

A matrix-valued function $Q_x : [0,T] \to \mathbb{S}_+^{n_x}$ describing an ellipsoidal tube enclosure $\overline{\Delta}(t) := \mathcal{E}(Q_x(t)) \supseteq \Delta(t)$ may be precomputed likewise. One approach involves determining ellipsoidal enclosures for the uncertainty-dependent terms in (7) using ellipsoidal calculus (Kurzhanski and Vályi, 1994; Villanueva et al., 2015b),

$$\forall (d_x, d_w, \hat{x}) \in \mathcal{E}(Q_x(t)) \times \Gamma \times \hat{X}(t),$$
$$d_\Omega(t)(\hat{x}(t) + d_x(t)) + F_w d_w(t) \in \mathcal{E}(\overline{Q}(t))\,,$$

and then propagating Q_x through the auxiliary ODEs:

$$\text{a.e. } t \in [0,T],$$
$$\dot{Q}_x(t) = (F_x + \hat{\Omega}) Q_x(t) + Q_x(t)(F_x + \hat{\Omega})^{\mathsf{T}} + \kappa(t) Q_x(t) + \frac{1}{\kappa(t)} \overline{Q}(t)$$
$$\text{with} \quad Q_x(0) = 0 \quad \text{and} \quad \kappa(t) := \sqrt{\frac{\mathrm{Tr}(\overline{Q}(t))}{\mathrm{Tr}\,(Q_x(t)) + \epsilon}}\,.$$

Another, potentially tighter, approach to propagating Q_x is based on the recent work on linear control systems with multiplicative uncertainty by Houska et al. (2016).

5. NUMERICAL CASE STUDY

We consider a fluidized catalytic cracking (FCC) unit operated in partial combustion mode (Hovd and Skogestad, 1993). The objective is to steer the system to a given operating point, defined in terms of the mass fraction of coke on regenerated catalyst, C_{rc}, and the regenerator dense bed temperature, T_{rg}. The manipulated variables are the flow rate of air sent to the regenerator, F_{a}, and the catalyst flow rate, F_{s}. A linear input-output dynamic model is obtained via linearization and reduction of a first-principles nonlinear model around the equilibrium point $C_{\mathrm{rc}}^* = 5.207 \times 10^{-3}$, $T_{\mathrm{rg}}^* = 965.4\,\mathrm{K}$, $T_{\mathrm{ro}}^* = 776.9\,\mathrm{K}$, $T_{\mathrm{cy}}^* = 988.1\,\mathrm{K}$, and $T_{\mathrm{f}}^* = 400\,\mathrm{K}$, where T_{f} denotes the feed oil temperature. The control and state variables in this linear dynamic system are

$$x(t) := \begin{bmatrix} C_{\mathrm{rc}}(t) - C_{\mathrm{rc}}^* \\ T_{\mathrm{rg}}(t) - T_{\mathrm{rg}}^* \end{bmatrix}, \qquad u(t) := \begin{bmatrix} F_{\mathrm{s}}(t) - F_{\mathrm{s}}^* \\ F_{\mathrm{a}}(t) - F_{\mathrm{a}}^* \end{bmatrix}.$$

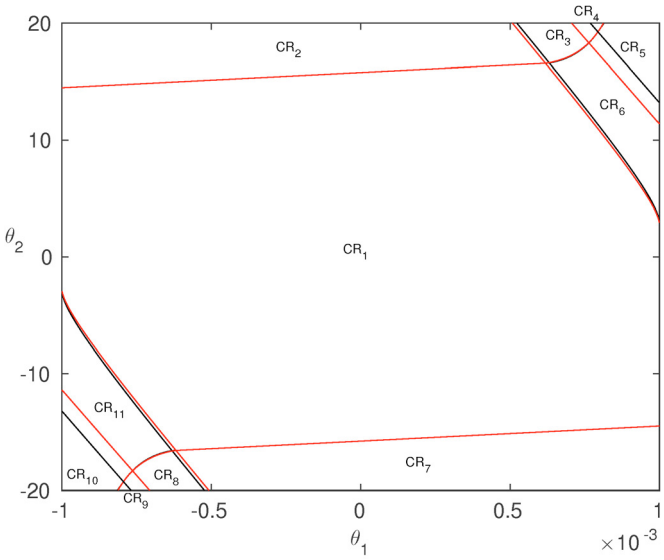

Fig. 2. Critical regions of the mp-DO. Black lines: nominal regions; Red lines: robust regions.

This optimization-based control problem complies with the formulation in (1), where the parameters θ correspond to uncertainty in the initial values of C_{rc} and T_{rg}, with $\Theta = [-10^{-3}, 10^{-3}] \times [-20, 20]$. Numerical values for this case study are reported in Appendix B.

A comparison of the critical regions of the mp-DO in the nominal case (with $F_w = 0$) and the robust case (with $w(t) \in W := [-5, 5]$) is shown in Fig. 2. Eleven regions are obtained in both cases:

- The critical region CR_1 corresponds to unconstrained optimal controls.
- The solutions in CR_2 and CR_7 are comprised of two arcs, a boundary arc where u_2 reaches its lower and upper bound, respectively, followed by an interior arc.
- The solutions in CR_6 and CR_{11} are comprised of three arcs, with a boundary arc where x_1 reaches its upper and lower bound, respectively, located in-between two interior arcs.
- In CR_5 and CR_{10}, the solutions have the same constrained arc as CR_6 and CR_{11}, respectively, yet without the final interior arc as the state constraint remains active until the terminal time.
- The solutions in CR_3 and CR_8 combine the previous two cases in CR_2+CR_6 or CR_7+CR_{11}, and give rise to four arcs, starting with a boundary arc for u_2 (like CR_2 or CR_7), followed by an interior arc, a boundary arc for x_1 (like CR_6 or CR_{11}), and a final interior arc.
- In CR_4 and CR_9, the solutions present the same structure as CR_3 and CR_8, respectively, but lack the final interior arc after the boundary arc for x_1.

The robust regions computed with either interval or ellipsoidal tube back-offs happen to be nearly identical in this case. The main effect of the back-offs is seen in the lower-left and upper-right corners, where the regions CR_4, CR_5, CR_9 and CR_{10}, and to a lesser extend the regions CR_3, CR_6, CR_8 and CR_{11}, are enlarged due to the state constraints being tightened.

The pre-computed ellipsoidal reachability tube (green line) is shown in Fig. (3(a)), here centered at a state reference

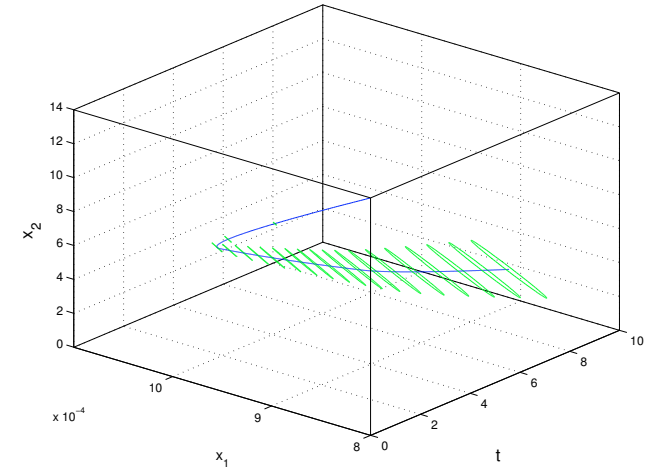

(a) Ellipsoidal reachability tube

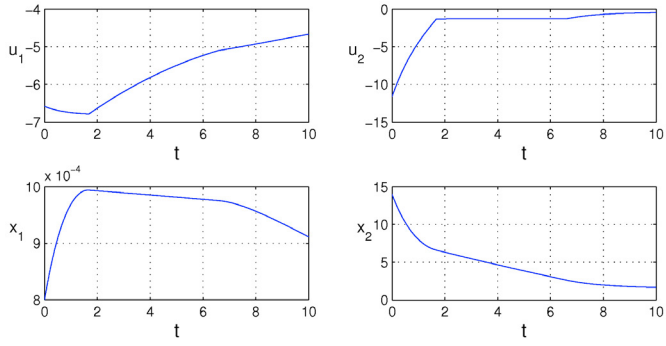

(b) Robust control and response trajectories

Fig. 3. Robust mp-DO based on ellipsoidal reachability tubes – Case of additive disturbance.

trajectory (blue line) originating from the initial state $x(0) = [8 \times 10^{-4}, 14] \in \mathsf{CR}_6$. Quite expectedly, this tube is found to grow along time due to the cumulated uncertainty. The effect of using this back-off is shown in Fig. 3(b), where the state x_1 is seen to remain away from its upper bound of 10^{-3}.

Closed-loop simulations obtained by applying both the nominal and robust mp-NCO-tracking controllers with a sampling period of $\Delta T = 1$ are shown in Fig. (4), for a given random disturbance $w(t) \in [-5, 5]$. It can be seen that the robust controller keeps the response feasible at all times, whereas some constraint violations are obtained with the nominal controller, for instance around $t = 6$.

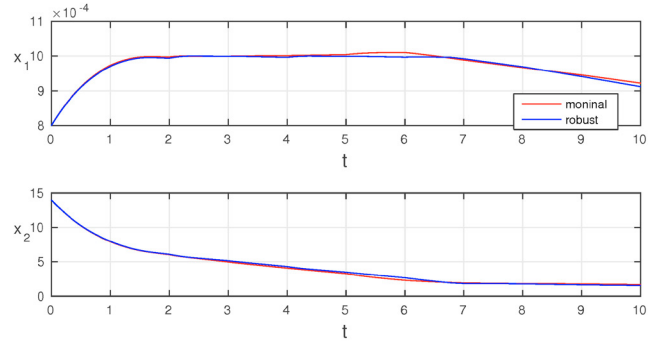

Fig. 4. Closed-loop performance of the nominal and robust mp-NCO-tracking controllers – Case of additive disturbance.

Finally, we illustrate the applicability of the methodology in the case of multiplicative uncertainty with $\Omega(t) \in [-0.1, 0.1]$ abs (F_x), and $F_w = 0$. A breakdown of the parameter space into 11 critical regions is obtained, similar to the one shown in Fig. 2. Here, ellipsoidal reachability tubes are found to be much less conservative than their interval counterparts nonetheless, due to the inability of the latter to handle the wrapping effect during the enclosure propagation. A set of robust control and response trajectories for the initial state $x(0) = [8 \times 10^{-4}, 14] \in \mathsf{CR}_6$ are shown in Fig. 5(a), where the back-offs are derived from ellipsoidal reachability tubes. Corresponding closed-loop simulations obtained by applying both the nominal and robust mp-NCO-tracking controllers with a sampling period of $\Delta T = 1$ are shown in Fig. 5(b), for a given random disturbance $\Omega(t) \in [-0.1, 0.1]$. Like previously, the robust controller keeps the response feasible at all times, whereas the nominal controller fails to enforce feasibility.

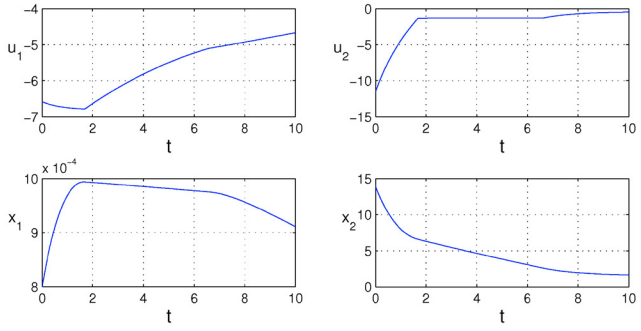

(a) Robust control and response trajectories

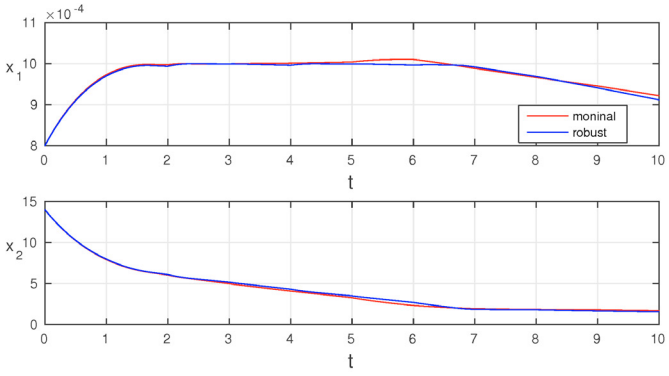

(b) Closed-loop mp-NCO-tracking control

Fig. 5. Robust mp-DO and mp-NCO-tracking controller performance – Case of multiplicative disturbance and ellipsoidal reachability tubes.

6. CONCLUSIONS

This paper has presented an extension of the mp-NCO-tracking approach by Sun et al. (2016) for the design of robust multi-parametric controllers for continuous-time linear dynamic systems subject to time-varying uncertainty. This extension involves backing-off of the path and terminal state constraints based on a worst-case uncertainty propagation in the form of interval and ellipsoidal reachability tubes. An inherent advantage of the approach is that the back-offs can be computed prior to solving the mp-DO problem, thus enabling the direct application of the controller design procedure in Sun et al. (2016) and

making the off-line computational effort independent of the number of uncertain parameters. The effect of backing-off of the constraints is a modification of the size of the critical regions, and possibly the number of critical regions too—either removing or adding extra regions. The applicability of the approach has been demonstrated by the case study of an FCC unit, considering either additive or multiplicative uncertainty. Future work will consider applications to higher-dimensional problems, where model reductions techniques may be used for reducing the order of the dynamic system subject to an acceptable performance loss (Pistikopoulos, 2012).

ACKNOWLEDGEMENTS

M. Sun thanks the Department of Chemical Engineering and the Faculty of Engineering of Imperial College London for an EPSRC International Doctoral Training Award (DTA). Financial support from Texas A&M University is gratefully acknowledged.

REFERENCES

Bemporad, A. and Morari, M. (1999). Robust model predictive control: A survey. *Lecture Notes in Control and Information Sciences*, 245, 207–226.

Bonvin, D. and Srinivasan, B. (2013). On the role of the necessary conditions of optimality in structuring dynamic real-time optimization schemes. *Computers & Chemical Engineering*, 51, 172–180.

Chachuat, B., Houska, B., Paulen, R., Perić, N., Rajyaguru, J., and Villanueva, M.E. (2015). Set-theoretic approaches in analysis, estimation and control of nonlinear systems. *IFAC-PapersOnLine*, 48(8), 981–995.

Houska, B., Mohammadi, A., and Diehl, M. (2016). A short note on constrained linear control systems with multiplicative ellipsoidal uncertainty. *IEEE Transactions on Automatic Control*, 61(12), 4106–4111.

Houska, B., Logist, F., Impe, J.V., and Diehl, M. (2012). Robust optimization of nonlinear dynamic systems with application to a jacketed tubular reactor. *Journal of Process Control*, 22(6), 1152–1160.

Hovd, M. and Skogestad, S. (1993). Procedure for regularity control structure selection with application to the FCC process. *AIChE Journal*, 39(12), 1938–1953.

Kadam, J.V., Schlegel, M., Srinivasan, B., Bonvin, D., and Marquardt, W. (2007). Dynamic optimization in the presence of uncertainty: From off-line nominal solution to measurement-based implementation. *Journal of Process Control*, 17, 389–398.

Kouramas, K.I., Panos, C., Faísca, N.P., and Pistikopoulos, E.N. (2013). An algorithm for robust explicit/multi-parametric model predictive control. *Automatica*, 49, 381–398.

Kurzhanski, A.B. and Vályi, I. (1994). *Ellipsoidal Calculus for Estimation and Control*. Birkhäuser, Boston.

Mayne, D.Q., Seron, M. M. and Raković, S. (2005). Robust model predictive control of constrained linear systems with bounded disturbances. *Automatica*, 41, 219–224.

Pistikopoulos, E.N. (2012). From multi-parametric programming theory to MPC-on-a-chip multi-scale systems applications. *Computers & Chemical Engineering*, 47, 57–66.

Rawlings, J.B. and Mayne, D.Q. (2009). *Model Predictive Control: Theory and Design*. Nob Hill Publishing.

Sakizlis, V., Kakalis, N.M.P., Dua, V., Perkins, J.D., and Pistikopoulos, E.N. (2004). Design of robust model-based controllers via parametric programming. *Automatica*, 40(2), 189–201.

Smith, R.S. (2004). Robust model predictive control of constrained linear systems. In *Proceedings of the 2004 American Control Conference*, 245–250.

Sun, M., Chachuat, B., and Pistikopoulos, E.N. (2016). Design of multi-parametric NCO tracking controllers for linear dynamic systems. *Computers & Cheminal Engineering*, 92, 64–77.

Villanueva, M.E., Houska, B., and Chachuat, B. (2015a). Unified framework for the propagation of continuous-time enclosures for parametric nonlinear ODEs. *Journal of Global Optimization*, 62, 575–613.

Villanueva, M.E., Rajyaguru, J., Houska, B., and Chachuat, B. (2015b). Ellipsoidal arithmetic for multivariate systems. *Computer Aided Chemical Engineering*, 37, 767–772.

Appendix A. SET NOTATION

The sets of compact and convex subsets of $\mathbb{R}^n$ are denoted by $\mathbb{K}^n$ and $\mathbb{K}^n_{\mathrm{C}}$. The set of n-dimensional symmetric positive semidefinite (resp. positive definite) matrices is denoted by $\mathbb{S}^n_+$ (resp. $\mathbb{S}^n_{++}$).

An interval vector is denoted by $\left[y^{\mathrm{L}}, y^{\mathrm{U}}\right]$, and its radius and midpoint are defined as:

$$\operatorname{mid}\left(\left[y^{\mathrm{L}}, y^{\mathrm{U}}\right]\right) := \frac{\left(y^{\mathrm{U}} + y^{\mathrm{L}}\right)}{2}, \tag{A.1}$$

$$\operatorname{rad}\left(\left[y^{\mathrm{L}}, y^{\mathrm{U}}\right]\right) := \frac{\left(y^{\mathrm{U}} - y^{\mathrm{L}}\right)}{2}. \tag{A.2}$$

An ellipsoid with center $q \in \mathbb{R}^n$ and shape matrix $Q \in \mathbb{S}^n_+$ is denoted by

$$\mathcal{E}(q,Q) := \left\{ q + Q^{\frac{1}{2}} v \;\middle|\; v \in \mathbb{R}^n, v^{\mathsf{T}} v \leq 1 \right\}, \tag{A.3}$$

or simply $\mathcal{E}(Q)$ when centered at the origin.

The support function $V[Z] : \mathbb{R}^n \to \mathbb{R}$ of a set $Z \in \mathbb{K}^n$ is

$$\forall c \in \mathbb{R}^n, \quad V[K](c) := \max_z \{ c^{\mathsf{T}} z \,|\, z \in Z \}. \tag{A.4}$$

In particular, the support functions of the interval $\left[y^{\mathrm{L}}, y^{\mathrm{U}}\right]$ and the ellipsoid $\mathcal{E}(q,Q)$ are defined for each $c \in \mathbb{R}^n$ as

$$V[\mathcal{E}(q,Q)](c) = c^{\mathsf{T}} q + \sqrt{c^{\mathsf{T}} Q c} \tag{A.5}$$

$$V[y^{\mathrm{L}}, y^{\mathrm{U}}](c) = c^{\mathsf{T}} \operatorname{mid}\left(\left[y^{\mathrm{L}}, y^{\mathrm{U}}\right]\right) + \operatorname{abs}(c)^{\mathsf{T}} \operatorname{rad}\left(\left[y^{\mathrm{L}}, y^{\mathrm{U}}\right]\right) \tag{A.6}$$

with $\operatorname{abs}(c) := (|c_1|, \ldots, |c_n|)^{\mathsf{T}}$.

The ith row (resp. column) of a matrix $A \in \mathbb{R}^{n \times n}$ is denoted by $A_{(i,\cdot)}$ (resp. $A_{(\cdot,i)}$).

Let $I \subset \mathbb{R}$, $\mathbb{L}^{n_u}_2(I)$ denotes the set of $\mathbb{L}_2$-integrable vector-valued functions of dimension n_u on I, and $\mathbb{W}^{n_x}_{1,2}(I)$, the set of n_x-dimensional weakly differentiable functions on I, whose weak derivative is $\mathbb{L}_2$-integrable.

Appendix B. CASE STUDY DATA

The equilibrium point is $C^*_{\mathrm{rc}} = 5.207 \times 10^{-3}$, $T^*_{\mathrm{rg}} = 965.4\,\mathrm{K}$, $T^*_{\mathrm{ro}} = 776.9\,\mathrm{K}$, $T^*_{\mathrm{cy}} = 988.1\,\mathrm{K}$, and $T^*_{\mathrm{f}} = 400\,\mathrm{K}$, where T_{f} denotes the feed oil temperature.

The non-zero matrices in the objective function and linear dynamic system of the optimal control problem (1) are:

$$Q_{\mathrm{f}} = \begin{bmatrix} 3.011 \times 10^7 & 1334 \\ 1334 & 1.260 \end{bmatrix}, \quad Q = \begin{bmatrix} 10^8 & 0 \\ 0 & 1 \end{bmatrix}, \quad R = \begin{bmatrix} 1 & 0 \\ 0 & 1 \end{bmatrix},$$

$$F_x = \begin{bmatrix} -2.55 \times 10^{-2} & 1.51 \times 10^{-6} \\ 227 & -4.10 \times 10^{-2} \end{bmatrix},$$

$$F_u = \begin{bmatrix} 3.29 \times 10^{-6} & -2.60 \times 10^{-5} \\ -2.8 \times 10^{-2} & 7.80 \times 10^{-1} \end{bmatrix}, \quad F_w = \begin{bmatrix} 6.87 \times 10^{-7} \\ 2.47 \times 10^{-2} \end{bmatrix}.$$

The path constraints are given by:

$$\begin{bmatrix} -100 \\ -15 \end{bmatrix} \leq u(t) \leq \begin{bmatrix} 100 \\ 15 \end{bmatrix}, \qquad \begin{bmatrix} -10^{-3} \\ -20 \end{bmatrix} \leq x(t) \leq \begin{bmatrix} 10^{-3} \\ 20 \end{bmatrix}.$$